Monatshefte für Chemie 135, 371–384 (2004)
DOI 10.1007/s00706-003-0132-z

Monatshefte für Chemie
Chemical Monthly
Printed in Austria

A DFT Study of Electron Structure, Geometry, and Keto–Enol Tautomerism of 3-Oxopropionyl Halogenides

Vassil B. Delchev*

University of Plovdiv, Department of Physical Chemistry, Plovdiv 4000, Bulgaria

Received August 19, 2003; accepted October 25, 2003
Published online February 2, 2004

Summary. The electronic and geometry structures of all enol and diketoforms of 3-oxopropionyl halogenides were investigated at the B3LYP/3-21G** level of theory. The comparative study of their energies revealed that the enol forms of the compounds are more stable than *cis*- and *trans*-diketones. All *cis*-diketones (except Cl-containing one) have one imaginary frequency in their vibration spectra, *i.e.* they do not correspond to local or global minima on the potential hypersurface. The keto–enol transformations enol $\rightleftarrows$ *cis*-diketone and enol $\rightleftarrows$ *trans*-diketone for a certain triad of tautomers/isomers pass through one transition state or in other words, the two conversions have one common maximum on the energy hypersurface. The energy barriers of the keto–enol conversions found for isolated molecules are quite high. Only for the enol $\rightarrow$ diketone conversions in solution the energy barriers are slightly reduced.

Keywords. *Ab initio*; B3LYP; Keto–enol; 3-Oxopropionyl halogenide.

Introduction

3-Oxopropionyl halogenides and malonaldehyde belong to the large group of β-dicarbonyl compounds. The mobility of the hydrogen atom linked up to the α-carbon atom determines a lot of interesting properties of these compounds from theoretical and experimental point of view. β-Diketones exist as two stable tautomers: enol and diketone. Depending on the conditions (temperature, solvent, physical condition, *etc.*) the two forms are transformed according to Scheme 1 (keto–enol tautomerism).

Two most important representatives of the β-diketones' group have been widely studied by theoretical and experimental methods [1, 2]. These are malonaldehyde [3] and acetylacetone [4, 5], which play an important role in organic synthesis. In this aspect, the composition with respect of enol and diketoform at certain conditions should be known. Two kinds of prototropic processes are

* Corresponding author. E-mail: vdelchev@hotmail.com

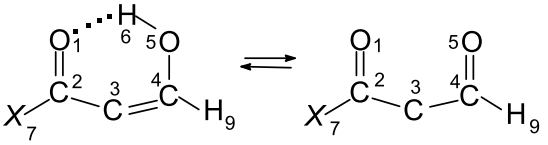

Scheme 1

observed in the equilibration of tautomeric forms of malonaldehyde, acetylacetone, and their derivatives: 1) a proton transfer between the two oxygen atoms in the enol form; and 2) a transformation of the enol form into diketone and *vice versa*. The first type of these prototropic processes has been well studied by theoretical and experimental techniques [6–14]. It has been found that the strength of the intramolecular hydrogen bond in the enol molecule directly affects the H-transfer rate and the energy barriers of the prototropic transformation [1]. As concerns the second type of prototropic processes, in most cases the mechanism of the hydrogen migration is known. In this aspect, several experimental investigations in the femtosecond and picosecond region have been reported [15–23]. However, for a large number of β-diketones these reactions have not been investigated so far.

Latajka et al. [15] have studied by means of *ab initio* methods the H-transfer in malonaldehyde in the ground state and in the first triplet excited state. According to their results the energy barrier of H-transfer in an excited state is higher than in the ground state. For 3-oxopropionyl halogenides similar investigations are not known so far. Furthermore, there aren't even data reported about the keto–enol equilibrium of these compounds.

The purpose of this paper is to investigate the kinetics of the keto–enol conversion of all 3-oxopropionyl halogenides in the gas phase passing through one transition state. The study involves a determination and characterization of the transition states and follows the reaction paths by means of the B3LYP functional.

Mainly discussions concerning the mechanism of the keto–enol tautomerism of malonaldehyde [24] and acetylacetone [25] are available up to now. The discussed mechanism involves one transition state (synchronous reaction), which is obtained by motion of the mobile hydrogen atom through space. The well known ''through-space'' mechanism has been proven to be the most probable one for β-diketones in the gas phase. Unfortunately, the influence of different solvent fields over the stability of the tautomeric forms and the reaction mechanism haven't been taken into account in Refs. [24, 25]. However, some experimental investigations [26] have shown that in a variety of solvents the configuration of the enol form is different. For example, in water a *trans*-enol configuration is available [25, 27], as well as in ethanol and diethyl ether [26, 28, 29], and in non-polar solvents like hexane the *cis*-enol configuration is the most stable one [26, 29]. It is also known that higher concentrations of the diketoform are measured in polar protic solvents [30–34] and *vice versa*. In this study the solvent effect was investigated with the Isodensity *Tomasi*'s Polarized Continuum Model (IPCM), which defines a cavity as an isodensity surface of the molecule. Here were used solvent fields generated by acetonitrile and chloroform molecules.

Results and Discussion

Enol- and Diketotautomers – Structure

In order to check the nature of the stationary points on the energy surface (global or local minima) we optimized all enols and diketones of 3-oxopropionyl halogenides and calculated their vibration spectra using the GAUSSIAN 98 program package [35].

The structures of the enol forms (in our further discussion they are designated with *E–X* where *X* replaces any halogen atom) correspond to minima on the energy surface because in their vibration spectra no negative *Hessian* coordinates (imaginary vibrations) were found. The stability of the enol forms results from the strong intramolecular H-bond available in their molecules. Due to this non-covalent bond all enols have S-*cis* configuration of the molecular skeleton. Thus, the oxygen and carbon atoms and the H(6) atom of each enol 3-oxopropionyl halogenide form a six-membered pseudoaromatic ring (see Fig. 1). The intramolecular H-bond is non-symmetrically situated between the two oxygen atoms and that's why the enol structures have considerably low symmetry – C_S. The same symmetry has been determined for malonaldehyde using higher basis sets [24, 32].

The internal coordinates given in Fig. 1 show that the lengths of the intramolecular H-bonds in enols are less than 2 Å. Comparing the bonds' length it is seen that the strongest intramolecular H-bond is formed in malonaldehyde as a result of its shortest length. Therefore, we should expect the keto–enol conversion of malonaldehyde to have the highest energy barrier.

The *trans*-diketostructures of 3-oxopropionyl halogenides, designated with *trans-K–X* (Fig. 1), were also assigned as minima on the potential energy surface. Opposite to the enol-forms, all *trans*-diketoforms have non-planar structures certainly because of the strong repulsion between the electron pairs of the oxygen atoms. This might be the reason that these atoms are situated at the longest distance. Otherwise, the energy of the intramolecular H-bond is higher than the repulsion energy of the oxygens' electron pairs. In this aspect, we expected preliminarily high energy barriers for all keto–enol conversions. Our attempts to find a linear correlation between *Pauling*'s electronegativity of the halogen atoms (taken from Ref. [36]) and the H-bond length failed.

In order to estimate the pure *cis-trans* isomerization energy during each keto–enol transformation we optimized also the structures of so-called *cis*-diketones, provided in Fig. 2.

Cis-diketones (*cis-K–X*, *X* is any halogen atom) have the same configuration of the skeleton like the enol forms with a substantial difference: the H(6) atom is bound to the C(3) atom and two C=O bonds are available. The planarity of these forms is responsible for their low symmetry – C_S (each *cis*-diketone has only one symmetry plane). The short distance between the oxygen atoms and absence of an intramolecular H-bond in *cis*-diketones are responsible for their low stability. They are less stable than all other tautomeric forms of 3-oxopropionyl halogenides examined so far. For example, *cis*-diketones do not correspond to local or global minima because in the vibration spectrum of each of them was calculated one imaginary frequency as a negative eigenvalue. The form of the vibration

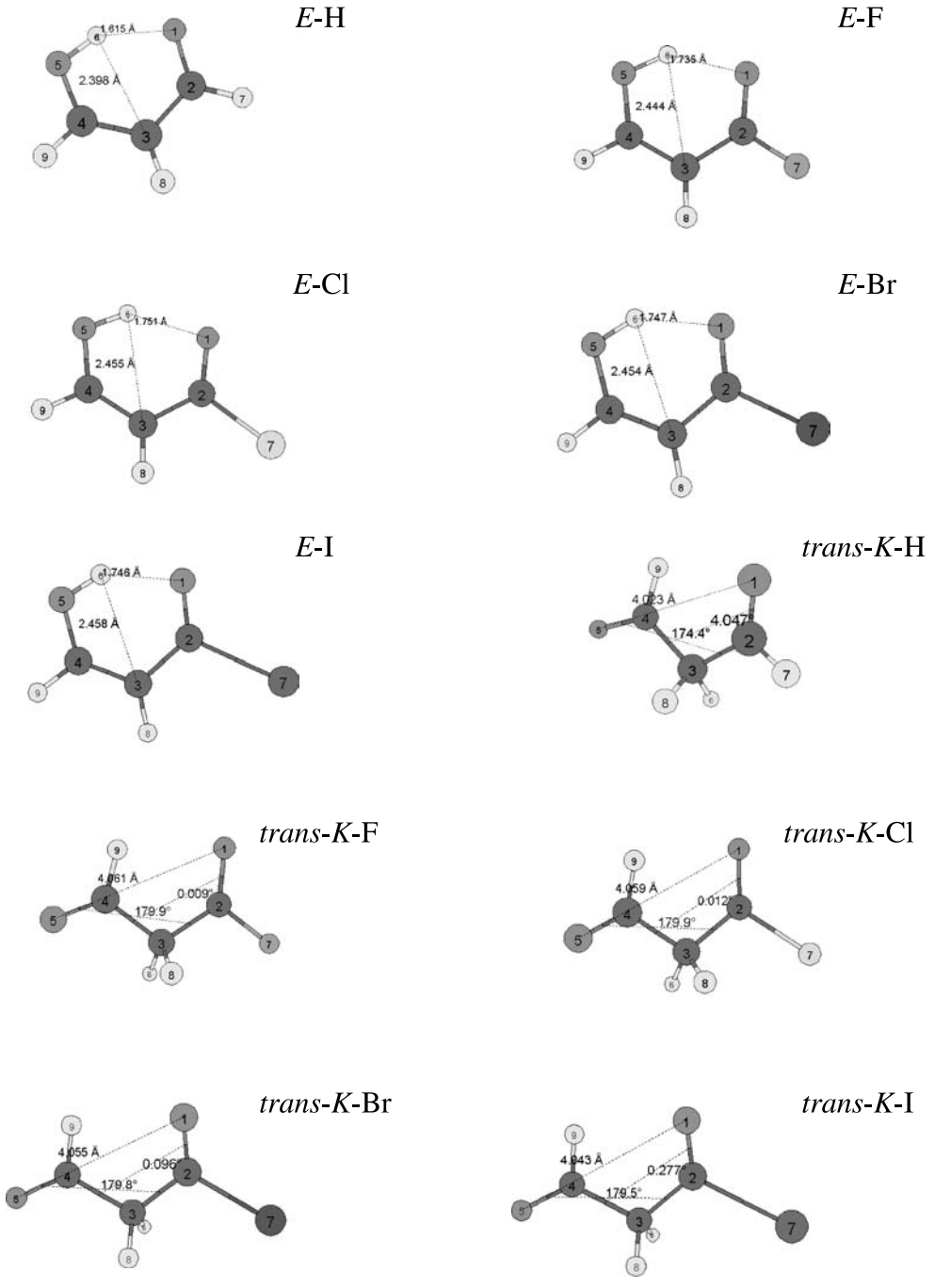

Fig. 1. Optimized enols (*E*–*X*) and diketones (*trans*-*K*–*X*) of 3-oxopropionyl halogenides; the structures were found as local minima, without imaginary frequencies in their vibration spectra

involved in this frequency is shown in Fig. 2 (see the second row of images). The eigenvectors show the preference of the molecules for *trans*-configuration and thus for stabilisation. All imaginary vibrations have low intensities, whose values in km mol^{-1} are given in brackets. Surprisingly, we found that the *cis*-*K*–Cl form

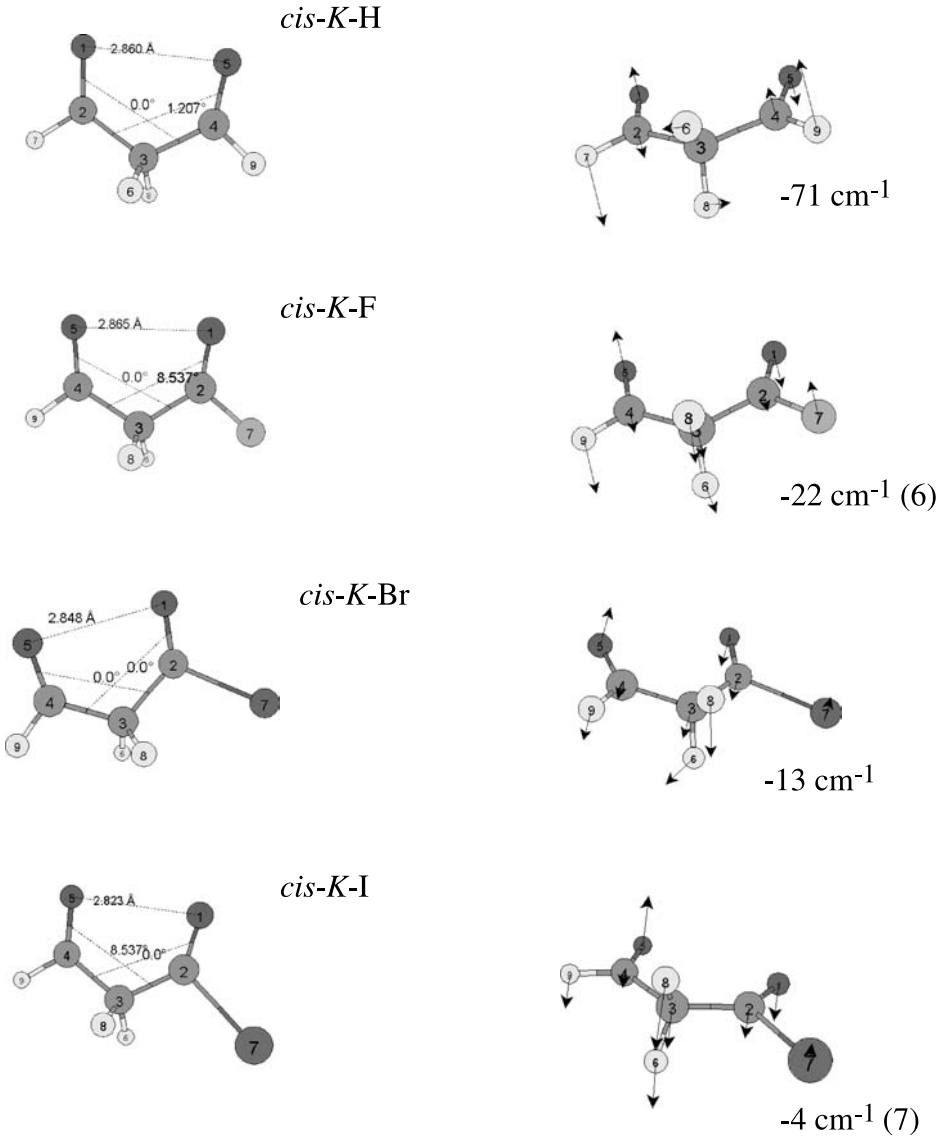

Fig. 2. *Cis*-diketoforms of 3-oxopropionyl halogenides; the right pictures represent eigenvectors of the imaginary frequency; the numbers in brackets show calculated IR intensities in km mol^{-1}

does not have any imaginary frequencies in the vibration spectrum, *i.e.* this tautomer forms a minimum on the energy hypersurface (see Fig. 3). We were not able to explain the reason for that but guessed that the *cis-K*–Cl form is a stable intermediate structure along the reaction path of the *E*–Cl → *trans-K*–Cl conversion.

In Table 1 calculated relative energies are given and the relative ZP corrected energies of all enols and diketoforms. The relative energies were calculated when the absolute energies of the enol forms (in Hartrees) were taken as conventional zeroes (these forms have the lowest energy). As concerns the diketoforms it is clear

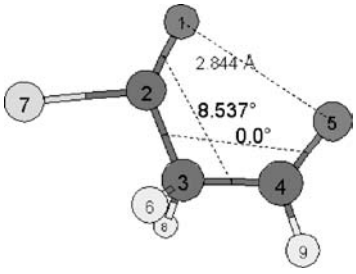

Fig. 3. The *cis-K*–Cl structure calculated without imaginary frequencies in the vibration spectrum (corresponding to a minimum)

Table 1. Relative energies (E) and relative ZP corrected energies ($E^o = E + \mathrm{ZP}E$) of 3-oxopropionyl halogenides, all in kJ mol^{-1}

Form	E					$E^o = E + \mathrm{ZP}E$				
	X=H	X=F	X=Cl	X=Br	X=I	X=H	X=F	X=Cl	X=Br	X=I
E–X	0[a]	0[b]	0[c]	0[d]	0[e]	0[f]	0[g]	0[h]	0[i]	0[j]
trans-K–X	73	62	60	60	60	64	54	52	52	52
cis-K–X	88	73	68	68	67	78	65	60	60	59
K–E–X	320	316	310	310	308	301	297	291	291	289

[a] The energies of the *E*–H form (−265.702185 Hartree); [b] *E*–F form (−364.417786 Hartree); [c] *E*–Cl form (−723.220724 Hartree); [d] *E*–Br form (−2827.153110 Hartree); [e] *E*–I form (−7155.743552 Hartree) and the sums $E + \mathrm{ZP}E$ of the [f] *E*–H form (−265.633421 Hartree); [g] *E*–F form (−364.356318 Hartree); [h] *E*–Cl form (−723.161060 Hartree); [i] *E*–Br form (−2827.093909 Hartree); [j] *E*–I form (−7155.684880 Hartree) were taken as conventional zeroes

that the *trans-K–X* forms are more stable than *cis-K–X* because of reasons explained above. The values from Table 1 confirmed that as well.

The vibration spectra of all forms were calculated. The frequencies are given as obtained from the calculations and they are not corrected with any scaling factor. The OH stretching vibrations in the enol structures are observed two times both mixed with C–H_9 stretchings ($\bar{\nu} = 3278$ and 2921 in *E*–H, 3308 and 3251 in *E*–F, 3317 and 3277 in *E*–Cl, 3313 and 3277 in *E*–Br, and 3313 and 3272 cm^{-1} in *E*–I). In other words, the two vibrations (O–H and C–H_9) have equal energy and close force constants. It is rather surprising that the OH stretching vibration appears over $\bar{\nu} = 3300$ cm^{-1} because, as it is known, usually it has to be at $\bar{\nu} = 2800$–3100 cm^{-1} due to the intramolecular H-bond influence. *E.g.* in the gas phase it is experimentally observed for acetylacetone at $\bar{\nu} = 2800$, and calculated at 3155 cm^{-1} [38]. The C=C and C=O stretching vibrations in the enol forms were calculated to reside in the intervals of $\bar{\nu} = 1662$–1612 and 1720–1643 cm^{-1}. It was found that an increase in the mass of the halogen substituent provokes a larger shift of the C=O and C=C frequencies towards smaller wavenumbers. The same regularity is observed for diketones for the C=O symmetric and asymmetric vibrations.

Table 2. *Mulliken* total atomic charges (*C*) of carbon atoms in the enol- and diketoforms (B3LYP/3-21G**)

Tautomeric form	q_{C2}	q_{C3}	q_{C4}
E–H	0.307	−0.308	0.248
E–F	0.676	−0.317	0.247
E–Cl	0.305	−0.258	0.249
E–Br	0.369	−0.264	0.245
E–I	0.301	−0.273	0.245
trans-K–H	0.321	−0.463	0.327
trans-K–F	0.661	−0.470	0.330
trans-K–Cl	0.324	−0.428	0.335
trans-K–Br	0.375	−0.430	0.332
trans-K–I	0.315	−0.438	0.331

Charge Distribution

In Table 2 we have provided the *Mulliken* total atomic charges of the carbon atoms which give a passing glance for the electron density distribution in the molecules of enols and diketones. On the other hand, they are a qualitative indicator for the reactions in which these compounds participate. The charges were computed together with the molecular geometries.

According to the data from Table 2 the *Mulliken* total atomic charge of C(2) (designated with q_{C2} and describing the ability of the compound to participate in nucleophilic reactions) is highest for the fluorine and lowest for the iodine compounds. Moreover, the q_{C2} charge in the fluorine compounds is about twice as high as in the other molecules. These may be results from the considerably high electronegativity of the F atom (3.98 [36]) as compared to the other halogens. We weren't able to explain why the electronegativity ratio, as *e.g.* of the fluorine and chlorine atom, is 1:0.80 while the ratio between their q_{C2} is only 1:0.45.

As concerns the electron density at the C(4) atom one can see from Table 2 that it is higher in the enol-forms *versus* the diketoforms. The reason is probably, the existing π-conjugation in the enol-forms, which causes an even distribution of the electron density. Conversely, the partial negative charge q_{C3} of the C(3) atom is higher in diketoforms. According to the q_{C3} values (Table 2) we expect the fluorine compounds to have the highest CH-acidity.

Keto–Enol Conversion Mechanisms

One preferred mechanism of keto–enol tautomerism between *E–X* and *trans-K–X* forms and between *E–X* and *cis-K–X* forms was examined. It involves motion of the H(6) atom through space between the O(5) and C(3) atoms, *i.e.* a case of an *antara*-migration of the proton. The mechanism involves one transition state between the tautomeric forms and has been proven to be the most probable one for β-diketones in the gas phase considering the rules for conservation of orbital symmetry [34, 37].

Studying this mechanism for our compounds we established, to our surprise, that each keto–enol conversion *E–X* $\rightleftarrows$ *trans-K–X* and E–X $\rightleftarrows$ *cis-K–X* passes through

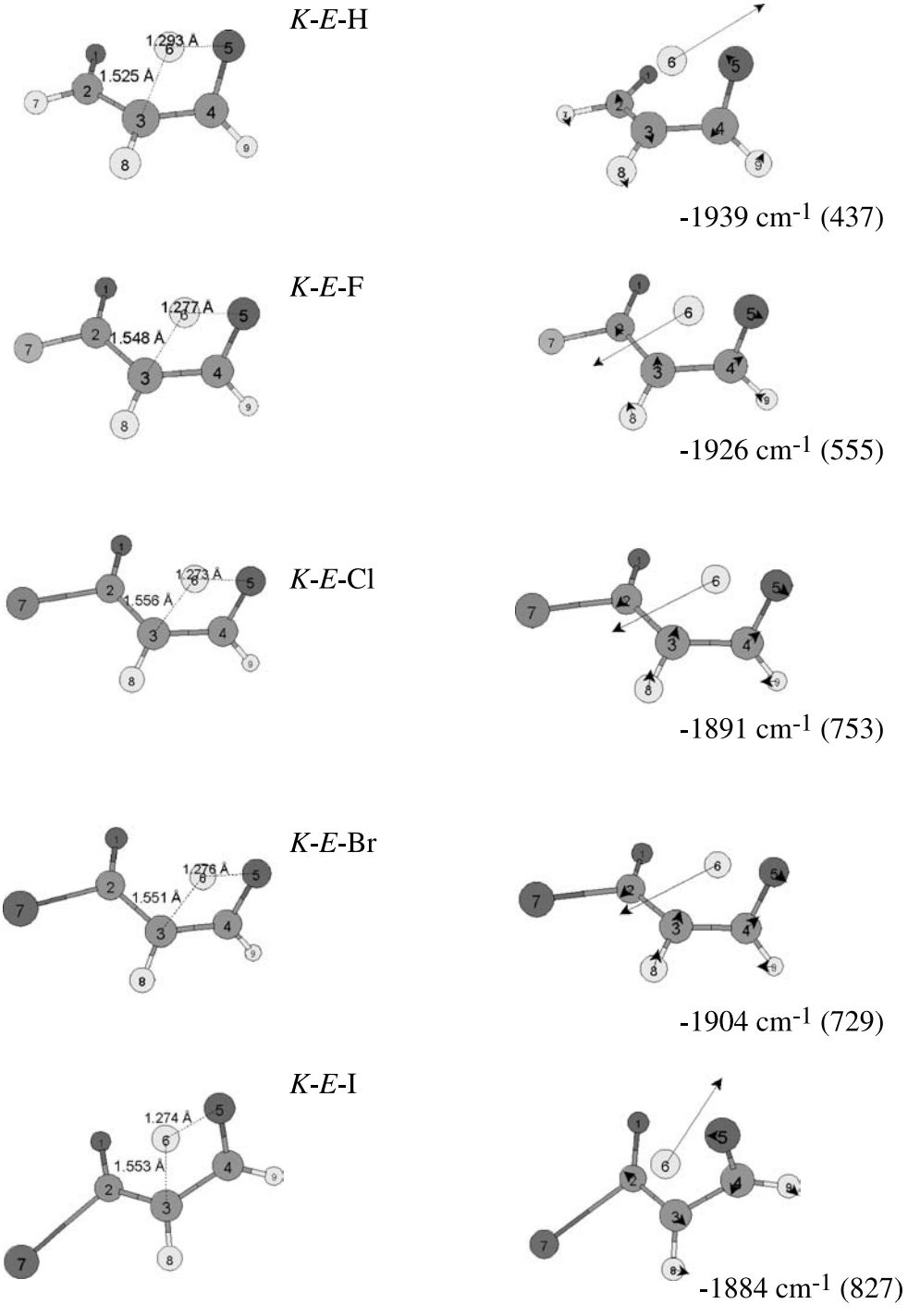

Fig. 4. Transition states (first order saddle points) of 3-oxopropionyl halogenides *cis-trans* keto–enol conversions; the right pictures illustrate the parallel modes of the imaginary vibrations; the numbers in brackets show calculated IR intensities in km mol^{-1}

one common transition state (the structures of transition states are shown in Fig. 4). It is seen that the transition states have non-planar geometries, which leads to the conclusion that even during the *E–X* $\rightleftarrows$ *cis-K–X* conversion the hydrogen migration occurs out of the molecular plane, in contrast with our preliminary expectations. During the conversion the planar structure of the enol-form is disturbed. After passing through the transition state towards *cis*-diketone it is restored again. Using this fact we estimated the energies of the pure *cis-trans* isomerizations ($E^{\text{cis-trans}}$) as the energy difference between the *cis*- and *trans*-diketones. They will be discussed below.

The non-planarity of the transition states is responsible for their low symmetry – C_1. In the vibration spectrum of each transition state one parallel mode was calculated as a negative eigenvalue (an imaginary frequency). In other words, the transition states were assigned as first order saddle points on the energy surface. The form of each parallel mode (see Fig. 4) reproduces the proton transfer between the enol-form and the diketoform. On the other hand, the parallel modes have the highest intensities as compared to the perpendicular modes of the transition states. The high absolute values of the imaginary frequencies and their intensities imply a sharp maximum (saddle) of each energy curve. Moreover, in both directions along the reaction coordinate the saddles are characterized with a large negative energy gradient.

In order to get a better concept about the energy curves we performed IRC calculations in both directions with all transitions states. By default, the calculation for one conversion took 6 steps in each direction from the transition state in steps of 0.1 $\text{amu}^{1/2}$ Bohr along the path. Each step corresponds to a geometry optimization and for each we obtained the internal coordinates of the modified transition state. In Table 3 the interesting *cis-trans* isomerization process space angles $D_1(C_2C_3C_4O_5)$ and $D_2(C_2E_3C_4H_6)$ are listed. The large change of these angles around the transition states proved that the hydrogen transfer occurs out of the molecular plane accompanied with a *cis-trans* isomerization of the molecular skeleton.

In order to clarify the nature of the transition states involved in the tautomerizations we performed subsequent PES scans of the reaction surfaces around the transition states. These calculations began from the transition state downhill towards the stable enol- and diketoform as 256 points on the hypersurface were computed for each reaction. Besides two distances (H(6)C(3) and H(6)O(5)) no other internal coordinates of the transition states were varied. The remaining internal coordinates were kept constant.

In Fig. 5 the transition-state-located potential hypersurfaces of 3-oxopropionyl halogenides (without malonaldehyde) are presented. Because the appearance of all surfaces is nearly the same we gave four different profiles, one for each conversion. The pale-gray regions have the lowest energy and the dark-gray the highest. The profiles have clearly shaped narrow ''slits'' that form a ''canyon''. Obviously, the reaction path passes through the ''slit'' and on its way gets over only one ''hill'', which corresponds to the transition state. Scanning only the area around the transition state does not allow to see the minimum of the *cis-K*–Cl form. We believe that such a minimum can be seen next to the minimum of the *trans-K*–Cl form or on the reaction path downhill towards the minimum of the *trans-K*–Cl form.

Table 3. Space angles $D_1(C_2C_3C_4O_5)$ and $D_2(C_2C_3C_4H_6)$ and their change uphill and downhill from the transition state along the reaction path

K–*E*–H			*K*–*E*–F			*K*–*E*–Cl			*K*–*E*–Br			*K*–*E*–I		
ΔE	D_1	D_2	ΔE	D_1	D_2	ΔE	D_1	D_2	ΔE	D_1	D_2	ΔE	D_1	D_2
70	76.1	86.7	71	80.3	89.2	69	81.6	89.6	70	80.7	89.2	69	81.4	89.5
54	76.1	85.9	54	80.1	88.4	53	81.3	88.9	53	80.5	88.4	53	81.2	88.8
39	75.9	85.2	39	79.9	87.7	38	81.2	88.3	39	80.3	87.8	38	81.0	88.2
26	75.7	84.4	26	79.6	87.0	25	81.0	87.6	25	80.0	87.1	25	80.8	87.6
15	75.5	83.7	15	79.4	86.4	14	80.7	87.0	14	79.8	86.5	14	80.6	87.0
6	75.3	83.1	6	79.2	85.8	6	80.5	86.5	6	79.6	85.9	6	80.4	86.4
0[a]	74.9	81.9	0[b]	78.8	84.7	0[c]	80.1	85.4	0[d]	79.2	84.8	0[e]	80.0	85.4
7	74.6	80.8	6	78.4	83.6	6	79.7	84.5	6	78.8	83.8	6	79.6	84.4
15	74.3	80.3	14	78.1	83.1	14	79.5	84.0	14	78.5	83.3	14	79.3	83.9
26	74.1	79.7	25	77.9	82.6	24	79.2	83.5	24	78.3	82.8	24	79.1	83.4
38	73.8	79.2	36	77.6	82.0	35	78.9	82.9	35	78.0	82.3	35	78.8	82.9
50	73.5	78.6	48	77.2	81.5	46	78.5	82.4	47	77.6	81.7	46	78.4	82.4
62	73.2	78.0	59	76.8	80.9	57	78.1	81.8	58	77.2	81.2	56	78.0	81.8

All angles are in degrees; ΔE is the relative absolute value of the energy fall (in kJ mol^{-1}) uphill and downhill from the transition state; the energies of all transition states were taken as conventional zeros (its absolute values are [a] −265.58026, [b] −364.29724, [c] −723.10247, [d] −2827.03495, and [e] −7155.62628 Hartree)

It is worth mentioning that all saddles have about 18 kJ mol^{-1} higher energy than the barriers estimated with the QST3 transition state optimization option. But on the background of the otherwise high energy barriers it was accepted that this increase is in the frames of the error for determination of the transition state on the hypersurface.

The relative energies of the transition states are listed in Table 1 and in Table 4 the energy barriers of the tautomeric conversions found as the energy difference between transition state and corresponding 3-oxopropionyl halogenide form are given. According to these values the lowest energy barrier has the keto–enol conversion of the iodine tautomers. The highest energy barrier of the forward transformation has the *E*–H → *cis*(*trans*)-*K*–H conversion. The reason for that is the stronger intramolecular H-bond available in the malonaldehyde enol form *versus* all other enol forms. However, this tautomerization has the lowest energy barrier of the reverse reaction (*cis*(*trans*)-*K*–H → *E*–H).

As a whole, the energy barriers of the conversions are rather high from what follows that the keto–enol tautomerizations in the gas phase are energetically disfavoured. At the expense of the high energy barriers the *cis-trans* isomerization energies ($E^{\text{cis-trans}}$) of the diketoforms are quite low (see Table 4). The highest *cis-trans* isomerization energy was predicted for malonaldehyde caused by the strong intramolecular H-bond. As concerns other values they are considerably close and low. This would mean that the halogen atom in the molecule does not affect the isomerization barrier. Their values are more sensitive to the intramolecular hydrogen bond strength, which directly influences the isomerization process.

The keto–enol conversions of the first triad of compounds were studied also including several solvent fields (chloroform and acetonitrile). The IPC model

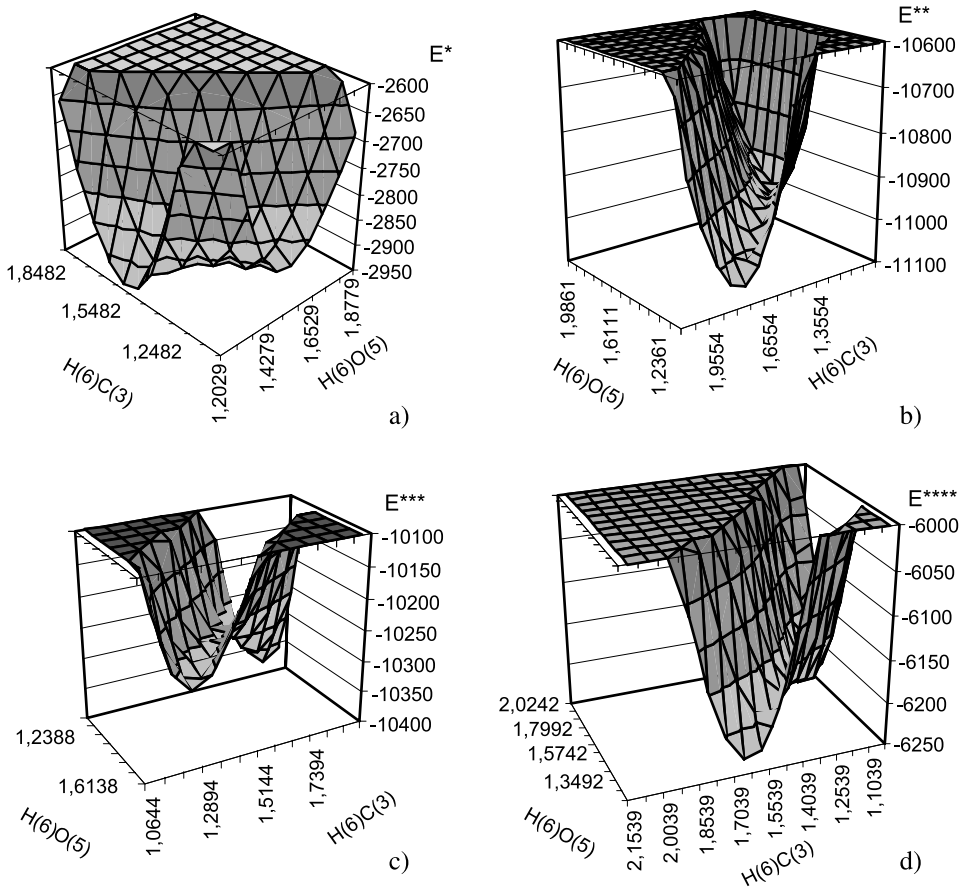

Fig. 5. 3D plots of energy surfaces of keto–enol conversions by the mechanism ''through-space'' for a) 3-oxopropionyl fluoride [$E^* = (E + 364) \times 10^4$ Hartree], b) 3-oxopropionyl chloride [$E^{**} = (E + 722) \times 10^4$ Hartree], c) 3-oxopropionyl bromide [$E^* = (E + 2826) \times 10^4$ Hartree], and d) 3-oxopropionyl iodide [$E^* = (E + 7155) \times 10^4$ Hartree]; on bottom of the 3D charts is given the dependence of H(6)C(3) *versus* H(6)O(5)

[39, 40] was used in order to estimate the change of the energy barriers in solution. They are given in Table 4. The values show a slight decrease *versus* the energy barriers in isolated state. Although the mechanism of the conversions in solution is different, it is believed for forward transformations that the probability of the ''through-space'' mechanism to occur is higher than in the isolated state. On the other hand, the reverse transformations in solution occur with higher energy barriers than in isolated state. Calculations of the mechanisms in solvents involving bromine and iodine compounds were not performed since they are rather time-consuming, but it is believed that the same trend will be observed.

The calculations for isolated molecules were repeated with the second order *Møller-Plesset* perturbation theory (*MP*2) and the same basis functions. The energy barriers, given in Table 4, are considerably higher than those obtained from

Table 4. Energy barriers and *cis-trans* isomerization energies ($E^{\text{cis-trans}}$)

	$X = E\text{–}X \rightleftarrows cis\text{-}K\text{–}X$							$X = E\text{–}X \rightleftarrows trans\text{-}K\text{–}X$				$E^{\text{cis-trans}}$	
	Forward				Reverse			Reverse					
	1	2	3	4	1	2	3	1	2	3	4	1	4
H	320	312	308	390	232	235	237	247	248	248	324	15	9
F	316	306	303	387	244	249	251	252	253	252	320	10	3
Cl	310	303	302	386	242	242	243	250	243	241	320	8	4
Br	310	–	–	384	242	–	–	250	–	–	321	8	4
I	308	–	–	383	240	–	–	248	–	–	319	8	3

All energies are in kJ mol^{-1}; [1] isolated molecules; [2] in chloroform; [3] in acetonitrile; [4] MP2/3-21G** calculations for isolated molecules

the B3LYP calculations. The average energy raising is about 72 kJ mol^{-1}. In contrast to that the *cis-trans* isomerization energies found with *MP2* are about 46% lower than the B3LYP ones. We tend to believe that the DFT gives much more reliable models of prototropic reactions than the *Møller-Plesset* perturbation theory.

Conclusions

The computations contributed to an elucidation of the relationship stability-structure of malonaldehyde and four 3-oxopropionyl halogenides. The computations revealed the mechanism of the keto–enol conversion of the compounds in the gas phase passing through one transition state. The following general conclusions were obtained:

- The enol forms of 3-oxopropionyl halogenides are more stable than the *cis*- and *trans*- diketones due to the stabilizing role of the intramolecular hydrogen bonds in their molecules.
- The strongest intramolecular hydrogen bond was found in the enol form of malonaldehyde. Obviously, the halogen atom in the remaining enol tautomers provokes an elongation of this bond and by this decreases its strength.
- *Cis*-diketoforms are unstable compared to *trans*-diketoforms. They do not correspond to minima because they possess imaginary frequencies in their vibration spectra. An exception is the *cis*-diketoform of 3-oxopropionyl chloride, which was assigned as an intermediate structure along the E–Cl $\rightarrow$ *trans-K*–Cl reaction pathway.
- Each *cis*-keto-/*trans*-keto–enol tautomeric–isomerization passes through one non-planar transition state. In other words all *cis*-keto–enol conversions occur with motion of the proton H(6) out of the molecular plane.
- The high energy barriers of the keto–enol conversions indicate that in the gas phase they occur with difficulty. According to the IPCM calculations non-protic solvents with different polarity like chloroform and acetonitrile provoke an insignificant decrease in the energy barriers of the forward reactions *versus* the gas phase.

Methods

The geometries of all compounds were fully optimized by *ab initio* methods at the B3LYP level using 3-21G** basis functions [35]. The calculated geometries were used in subsequent frequency calculations to prove that the rotamers correspond or do not correspond to energy minima in the full ($9\times3=27$ *Cartesian* coordinates, $27-6=21$ internal coordinates) coordinate hypersurface. The QST2 (using two geometries) and QST3 (using two geometries and a guess of the transition state), implemented within the GAUSSIAN 98 programme [35], were used to find the transition states (geometry and energy) between pairs of tautomers. Again, frequency calculations were used to prove that the transition states correspond to saddle points with one negative frequency. The frequency calculations also provided the zero-point energy corrections. IRC calculations of 13 points (6 uphill, 6 downhill from the saddle point, and one of the transition state) were performed to study the nature of the energy curve around the transition states. They were supported by SCAN calculations of the area nearest the transition state. The scan calculations were done by two internal coordinates: H(6)$\cdots$O(5) and C(3)$\cdots$H(6). Solvent inclusion calculations were done with the IPCM, which performed single point calculations of the optimized tautomers and transition states in solvent fields created by chloroform and acetonitrile.

Acknowledgements

The author thanks *H. Mikosch* and *G. Bauer* for the help connected with creation of an account on the TU-WIEN server where the calculations were performed.

References

[1] Buemi G, Gandolfo C (1989) J Chem Soc Faraday Trans 2 **85**: 215
[2] Andreassen AL, Bauer SH (1972) J Mol Struc **12**: 381
[3] Foresman JB, Frisch Æ (1995–1996) Exploring Chemistry with Electronic Structure Methods, 2nd ed. Gaussian
[4] Lowrey AH, George C, D'Antonio P, Karle J (1971) J Am Chem Soc **93**: 6399
[5] Schaefer JP, Wheatley PJ (1966) J Chem Soc A 528
[6] Luth K, Scheiner S (1994) J Phys Chem **98**: 3582
[7] Das K, Sarkar N, Majumdar D, Bhattacharyya K (1992) Chem Phys Lett **198**: 443
[8] Arthen-Engeland Th, Bultmann T, Ernsting N, Rodrigues MA, Thiel W (1992) Chem Phys **163**: 43
[9] Ernsting NP, Arthen-Engeland Th, Rodrigues MA, Thiel W(1992) J Chem Phys **97**: 3914
[10] Brinn IM, Carvalho CEM, Heisel F, Miehe JA (1991) J Phys Chem **95**: 6540
[11] Hoshimoto E, Yamauchi S, Hirota N, Nagaoka SJ (1991) J Phys Chem **95**: 10229
[12] Nagaoka S, Itoh A, Mukai K, Hoshimoto E, Hirota N (1992) Chem Phys Lett **192**: 532
[13] Dick B (1990) J Phys Chem **94**: 5752
[14] Waluk J, Bulska H, Grabowska A, Mordzinski A (1986) New J Chem **10**: 413
[15] Latajka Z, Scheiner S (1992) J Phys Chem **96**: 9764
[16] Barbara PF, Brus LE, Rentzepis PM (1986) J Am Chem Soc **102**: 5631
[17] Chou P-T, Martinez ML, Studer SL (1990) J Phys Chem **94**: 3639
[18] Brucker GA, Kelley DF (1988) J Phys Chem **92**: 3805
[19] Dick B, Ernsting NP (1987) J Phys Chem **91**: 4261
[20] Elsaesser T, Kaiser W (1986) Chem Phys Lett **128**: 231
[21] Heldt J, Gormin D, Kasha M (1989) Chem Phys **136**: 321
[22] Parthenopoulos DA, McMorrow D, Kasha M (1991) J Phys Chem **95**: 2668
[23] Rovira MC, Scheiner S (1995) J Phys Chem **99**: 9854

[24] Delchev VB, Nikolov G (2000) Monatsh Chem **131**: 99
[25] Delchev VB, Mikosch H, Nikolov G (2001) Monatsh Chem **132**: 339
[26] Bertz Steven H, Dabbagh G (1990) J Org Chem **55**: 5161
[27] George WO, Mensell VG (1968) J Chem Soc B **132**
[28] Brown RS, Tse A, Nakashima T, Haddon RC (1979) J Am Chem Soc **101**: 3157
[29] Noi RS, Ershov BA, Kol'tsov AI (1975) Zh Org Khim **11**: 1778
[30] Burdett JL, Rogers MT (1964) J Am Chem Soc **86**: 2105
[31] Rogers MT, Burdett JL (1965) Can J Chem **43**: 1516
[32] Delchev VB, Nikolov G (2000) Monatsh Chem **131**: 107
[33] Delchev VB, Mikosch H (2001) Monatsh Chem **132**: 223
[34] Nikolov GS, Markov P (1977/78) Annual of Sofia University **1**: 109
[35] Frisch MJ, Trucks GW, Schlegel HB, Scuseria GE, Robb MA, Cheeseman JR, Zakrzewski VG, Montgomery JA Jr, Stratmann RE, Burant JC, Dapprich S, Millam JM, Daniels AD, Kudin KN, Strain MC, Farkas O, Tomasi J, Barone V, Cossi M, Cammi R, Mennucci B, Pomelli C, Adamo C, Clifford S, Ochterski J, Petersson JA, Ayala PY, Cui Q, Morokuma K, Malick DK, Rabuck AD, Raghavachari K, Foresman JB, Cioslowski J, Ortiz JV, Stefanov BB, Liu G, Liashenko A, Piskorz P, Komaromi I, Gomperts R, Martin RL, Fox DJ, Keith T, Al-Laham MA, Peng CY, Nanayakkara A, Gonzalez G, Challacombe M, Gill PMW, Johnson B, Chen W, Wong MW, Andres JL, Gonzalez C, Head-Gordon M, Replogle ES, Pople JA (1998) Gaussian 98, A.3., Revision, Gaussian, Pittsburgh PA
[36] Emsley J (1993) The Elements, 2nd ed. Mir press, Moscow (in Russian)
[37] Nikolov GS, Markov P (1981) J Photochem **16**: 93
[38] Tayyari SF, Milani-nejad F (2000) Spectrochim Acta A **56**: 2679
[39] Miertus S, Scrocco E, Tomasi J (1981) Chem Phys **55**: 117
[40] Miertus S, Tomasi J (1982) Chem Phys **65**: 239